

RETRACTED: Dirac leptogenesis via scatteringsJulian Heeck^{1,*}, Jan Heisig^{2,1,†} and Anil Thapa^{1,‡}¹*Department of Physics, University of Virginia, Charlottesville, Virginia 22904-4714, USA*²*Institute for Theoretical Particle Physics and Cosmology, RWTH Aachen University, D-52056 Aachen, Germany* (Received 30 June 2023; accepted 10 August 2023; published 25 August 2023)

Leptogenesis typically requires the introduction of heavy particles whose out-of-equilibrium decays are essential for generating a matter-antimatter asymmetry, according to one of Sakharov's conditions. We show that, in Dirac leptogenesis, scatterings between the light degrees of freedom—Standard Model particles plus Dirac neutrinos—suffice to generate the asymmetry. Sakharov's conditions are satisfied because the right-handed neutrino partners are out of equilibrium. Consequently, heavy degrees of freedom never needed to be produced in the early Universe, allowing for a reheating temperature below their mass scale. We solve the Boltzmann equations and discuss the viable parameter space together with observational signatures such as an increased number of effective neutrinos in the early Universe as well as proton decay for some realizations.

DOI: [10.1103/PhysRevD.108.L031703](https://doi.org/10.1103/PhysRevD.108.L031703)**I. INTRODUCTION**

The indirect observation of nonzero neutrino masses via neutrino oscillations is proof of physics beyond the Standard Model (SM) and demands the introduction of new particles. So far, experiments have not been able to distinguish between the two qualitatively different possibilities of neutrinos being Dirac or Majorana particles.

Majorana neutrinos, especially when realized in a seesaw mechanism, often have the right ingredients for baryogenesis via leptogenesis [1,2]. Essentially, the $\Delta L = 2$ interactions that generate Majorana neutrino masses can create a lepton asymmetry in the early Universe that is then converted to a baryon asymmetry via sphalerons [3]. According to Sakharov's conditions [4], this not only requires lepton number and CP violation, but also out-of-equilibrium dynamics, usually satisfied through freeze-out or freeze-in of the heavy seesaw states. The simultaneous explanation of neutrino masses and the baryon asymmetry is a massive appeal of Majorana-neutrino models.

Alas, Dirac neutrinos too can generate a matter-antimatter asymmetry, as shown in Ref. [5]. Here, the smallness of the Dirac-neutrino mass term effectively decouples the

right-handed neutrino partners ν_R from the rest of the SM plasma. Even without ever breaking lepton number it is then possible to create an effective lepton asymmetry by hiding an opposite asymmetry in the ν_R sector [5]. Much like in the seesaw case, Sakharov's out-of-equilibrium condition is typically satisfied via heavy decaying particles [5,6].

However, since the ν_R are themselves out of equilibrium, Dirac leptogenesis can satisfy Sakharov's condition without the decay of heavy particles: $2 \rightarrow 2$ scatterings of SM particles and ν_R are sufficient to create a lepton asymmetry. Using the simple Dirac-leptogenesis models from Ref. [6], we show here that the observed baryon asymmetry, $Y_{\Delta B} \simeq 0.9 \times 10^{-10}$ [2,7], can be obtained even if the temperature of our Universe never reached the masses of the mediator particles.

In the literature one can find other scattering-induced baryogenesis scenarios in which the out-of-equilibrium particles are either part of some hidden sector [8] or (asymmetric) dark matter [9–13]. To the best of our knowledge, we are the first to propose the right-handed Dirac-neutrino partners for this role, which naturally have the desired properties.

The rest of this Letter is organized as follows: in Sec. II we briefly recap the simplest renormalizable Dirac-leptogenesis model and discuss the Boltzmann equations for the right-handed neutrinos in Sec. III. The CP asymmetry in $2 \rightarrow 2$ scattering is discussed in Sec. IV, where we also present the solutions to the Boltzmann equations. In Sec. V we discuss the baryon asymmetry generation in this model and the viable parameter space. Having focused on the simplest model, we discuss how other realizations would modify the results in Sec. VI. Finally, we conclude in Sec. VII.

*heck@virginia.edu†heisig@virginia.edu‡wtd8kz@virginia.edu

Published by the American Physical Society under the terms of the [Creative Commons Attribution 4.0 International license](https://creativecommons.org/licenses/by/4.0/). Further distribution of this work must maintain attribution to the author(s) and the published article's title, journal citation, and DOI. Funded by SCOAP³.

II. SIMPLE MODEL

For concreteness, we focus on the simple renormalizable Dirac-leptogenesis models from Ref. [6],¹ which can all successfully explain the observed baryon asymmetry under the assumption that the Universe was hot enough to create the mediators on shell. Here, we drop this implicit assumption and explore the opposite scenario: a Universe that was never hot enough to produce the heavy mediator particles, safe for a negligible number from the high-energy tails of the thermal distributions. Since the mediators are never on shell by assumption, we could equally well do away with them altogether and replace their effect by effective operators, similar to Ref. [16]. We follow the former path to facilitate direct comparison with the mediator decay case from Ref. [6].

In this spirit, let us focus our quantitative discussion on the minimal Dirac-leptogenesis realization [6], which supplements the SM by two electrically charged scalars $X_{1,2} \equiv X_{\bar{1},2}^-$ in addition to the three right-handed neutrinos ν_R necessary for massive Dirac neutrinos. The relevant interactions of $X_{1,2}$ are described by the Lagrangian

$$\mathcal{L} = \frac{1}{2} \bar{L}^c F_i L \bar{X}_i + \bar{e}^c G_i \nu_R \bar{X}_i + \text{H.c.}, \quad (1)$$

where X_i are assumed to be mass eigenstates with $M_1 < M_2$ and we suppress the flavor indices of $F_{1,2}$ and $G_{1,2}$. The full Lagrangian conserves baryon minus lepton number upon assigning $(B - L)(X_i) = -2$. While $B - L$ is hence conserved over the entire history of our Universe, ν_R number need not be, allowing sphalerons—which are blind to the ν_R —to convert the matching asymmetry $Y_{\Delta\nu_R} = Y_{\Delta(B-L_{\text{SM}})}$ into a baryon asymmetry [3,17]

$$Y_{\Delta B} = \frac{28}{79} Y_{\Delta(B-L_{\text{SM}})} = \frac{28}{79} Y_{\Delta\nu_R}. \quad (2)$$

The interactions in \mathcal{L} indeed break ν_R number if both F and G are nonzero, which can then produce a ν_R asymmetry as long as the processes also violate CP , as we show in the next section.

III. BOLTZMANN EQUATIONS

We consider the scenario that the reheating temperature T_{reh} is well below the charged scalar masses, $T_{\text{reh}} \ll M_1, M_2$, so the X_i abundance is virtually zero. Aside from the SM particles, which we assume to be in equilibrium, we then only need to track the ν_R in our Boltzmann equations. An asymmetry can be generated via $2 \rightarrow 2$ scatterings among the right-handed neutrinos and SM leptons. The respective s - and t -channel diagrams are shown in Fig. 1.

¹The same models were discussed in Refs. [14,15], albeit for Majorana neutrinos and thus with different phenomenology.

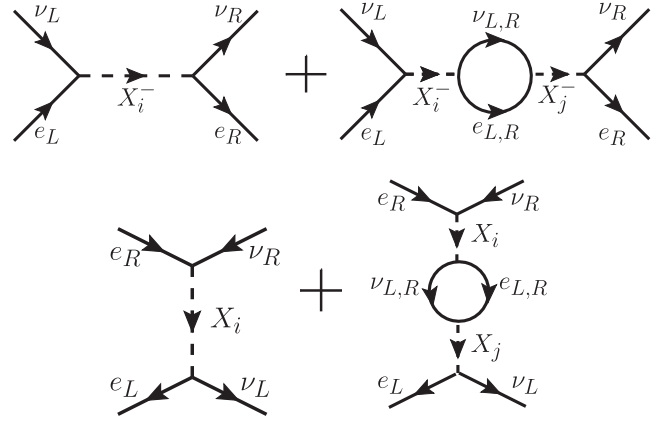


FIG. 1. Tree-level and one-loop wave-function diagram whose interference produces the CP -asymmetry ε_s (top) and ε_t (bottom).

We define the corresponding CP asymmetries $\varepsilon_s, \varepsilon_t$ via the thermally averaged cross sections, which are the relevant quantities for the Boltzmann equations:

$$\langle \sigma v \rangle_{\nu_R e_R \rightarrow LL} = \langle \sigma v \rangle_s (1 + \varepsilon_s), \quad (3)$$

$$\langle \sigma v \rangle_{\bar{\nu}_R \bar{e}_R \rightarrow \bar{L} \bar{L}} = \langle \sigma v \rangle_s (1 - \varepsilon_s), \quad (4)$$

$$\langle \sigma v \rangle_{\nu_R \bar{L} \rightarrow \bar{e}_R L} = \langle \sigma v \rangle_t (1 + \varepsilon_t), \quad (5)$$

$$\langle \sigma v \rangle_{\bar{\nu}_R L \rightarrow e_R \bar{L}} = \langle \sigma v \rangle_t (1 - \varepsilon_t). \quad (6)$$

The cross sections on the left-hand side are averaged (summed) over all initial (final) state flavors, and the thermal average is defined as usual by

$$\langle \sigma v \rangle_{12 \rightarrow 34} = \frac{g_1 g_2}{n_1 n_2} \left(\prod_{a=1}^4 \int \frac{d^3 p_a}{2E_a (2\pi)^3} \right) |\overline{\mathcal{M}}|^2 \quad (7)$$

$$\times f_1 f_2 (1 - f_3) (1 - f_4) \\ \times (2\pi)^4 \delta^4(p_1 + p_2 - p_3 - p_4),$$

$$\simeq \frac{g_1 g_2 T}{32\pi^4 n_1^{\text{eq}} n_2^{\text{eq}}} \int ds s^{3/2} \sigma(s) K\left(\frac{\sqrt{s}}{T}\right), \quad (8)$$

where g_a, f_a , and $n_a^{(\text{eq})}$ are the number of degrees of freedom, momentum distribution and (equilibrium) number density of particle a , respectively. The last line is obtained for vanishing (initial state particle) masses and Maxwell-Boltzmann distributions. In this case, $K(z)$ can be identified with the modified Bessel function of the second kind of order one. However, we can approximately describe Fermi-Dirac distributions for all particles except for the right-handed neutrino in the same way using $K(z)$ as defined in Ref. [18]. For small occupation numbers of the right-handed neutrino—justified in most of the parameter space of interest—the accuracy of this approximation is at the few percent level [18]. Notice that the s -channel cross section diverges when $s \simeq M_i^2$, i.e., as the X_i go on shell. Since $T_{\text{reh}} \ll M_1, M_2$ here, that region is heavily suppressed in

the integral, and we effectively restrict the cross section to the off-shell piece.

Disregarding the heavy scalars and defining $x \equiv T_{\text{reh}}/T$ as a measure of time, we can write the relevant Boltzmann equations for $\Sigma_{\nu_R} \equiv Y_{\nu_R} + Y_{\bar{\nu}_R}$ and $\Delta_{\nu_R} \equiv Y_{\nu_R} - Y_{\bar{\nu}_R}$ (where $Y_a = n_a/s$ denotes the comoving number density and we have summed over all flavors) as

$$\frac{d\Sigma_{\nu_R}}{dx} = \frac{1}{3\mathcal{H}} \frac{ds}{dx} \left[\frac{1}{2} \langle \sigma v \rangle_s \Sigma_{e_R}^{\text{eq}} (\Sigma_{\nu_R} - \Sigma_{\nu_R}^{\text{eq}}) + \frac{1}{2} \langle \sigma v \rangle_t \Sigma_L^{\text{eq}} (\Sigma_{\nu_R} - \Sigma_{\nu_R}^{\text{eq}}) \right], \quad (9)$$

$$\frac{d\Delta_{\nu_R}}{dx} = \frac{1}{3\mathcal{H}} \frac{ds}{dx} \left[\frac{1}{2} \langle \sigma v \rangle_s \{ \Delta_{\nu_R} (\Sigma_{\nu_R} + 2\Sigma_{\nu_R}^{\text{eq}} + \Sigma_{e_R}^{\text{eq}}) + \varepsilon_s \Sigma_{e_R}^{\text{eq}} (\Sigma_{\nu_R} - \Sigma_{\nu_R}^{\text{eq}}) \} + \frac{1}{2} \langle \sigma v \rangle_t \{ 2\Delta_{\nu_R} (\Sigma_{\nu_R} + \Sigma_{\nu_R}^{\text{eq}} + \Sigma_L^{\text{eq}}) + \varepsilon_t \Sigma_L^{\text{eq}} (\Sigma_{\nu_R} - \Sigma_{\nu_R}^{\text{eq}}) \} \right]. \quad (10)$$

Here, \mathcal{H} is the Hubble expansion rate and s the entropy density, not to be confused with the Mandelstam variable. Note that we have only kept terms linear in ε and Δ_{ν_R} . The Boltzmann equations in terms of Y_a that serve as a starting point for the derivation of Eqs. (9) and (10) can be found in the Appendix of Ref. [6].

Σ_{ν_R} tracks the total number of right-handed neutrinos, which is the relevant observable for N_{eff} , the number of effective neutrinos in the early Universe. Δ_{ν_R} on the other hand tracks the ν_R asymmetry we are interested in. A quick inspection shows that $\Delta_{\nu_R} = 0$ if $\varepsilon_{t,s} = 0$, as expected from Sakharov. However, since ε_t and ε_s are neither constant nor necessarily proportional to each other we cannot track a kind of efficiency $\Delta_{\nu_R}/\varepsilon$ as in decay scenarios. Luckily, the Boltzmann equations are easy to solve, even analytically in the limit where the X_i are integrated out.

IV. SCATTERING ASYMMETRY

The necessary CP asymmetries in our model arise at one loop through the simple diagrams of Fig. 1. The temperature-dependent asymmetries are defined here via the thermally averaged cross sections

$$\varepsilon_s = \frac{\langle \sigma v \rangle_{\nu_R e_R \rightarrow LL} - \langle \sigma v \rangle_{\bar{\nu}_R \bar{e}_R \rightarrow \bar{L} \bar{L}}}{\langle \sigma v \rangle_{\nu_R e_R \rightarrow LL} + \langle \sigma v \rangle_{\bar{\nu}_R \bar{e}_R \rightarrow \bar{L} \bar{L}}}, \quad (11)$$

$$\varepsilon_t = \frac{\langle \sigma v \rangle_{\nu_R \bar{L} \rightarrow \bar{e}_R L} - \langle \sigma v \rangle_{\bar{\nu}_R L \rightarrow e_R \bar{L}}}{\langle \sigma v \rangle_{\nu_R \bar{L} \rightarrow \bar{e}_R L} + \langle \sigma v \rangle_{\bar{\nu}_R L \rightarrow e_R \bar{L}}}. \quad (12)$$

In the limit of vanishing external-particle masses, the asymmetries read

$$\varepsilon_j = \frac{\int ds s^{3/2} \sigma_j^i(s) K(\sqrt{s}/T)}{2 \int ds s^{3/2} \sigma^j(s) K(\sqrt{s}/T)}, \quad j = s, t. \quad (13)$$

We define the positive semidefinite hermitian 2×2 matrices $\mathcal{F}_{ij} \equiv \text{tr}(F_i^\dagger F_j)$ and $\mathcal{G}_{ij} \equiv \text{tr}(G_i^\dagger G_j)$, which allow us to write

$$\sigma_-^s(s) = \frac{1}{64\pi^2} \left\{ \frac{s^2 \Im[\mathcal{F}_{12} \mathcal{G}_{21}](\mathcal{F}_{11} + \mathcal{G}_{11})}{(s - M_1^2)^2 (s - M_2^2)} + (1 \leftrightarrow 2) \right\}, \quad (14)$$

$$\sigma^s(s) = \frac{1}{16\pi} \left\{ \frac{s \mathcal{F}_{11} \mathcal{G}_{11}}{(s - M_1^2)^2} + (1 \leftrightarrow 2) \right\}, \quad (15)$$

$$\sigma_-^t(s) = \frac{1}{64\pi^2} \{ A(s, M_1, M_2) \Im[\mathcal{F}_{12} \mathcal{G}_{21}](\mathcal{F}_{11} + \mathcal{G}_{11}) + (1 \leftrightarrow 2) \}, \quad (16)$$

$$\sigma^t(s) = \frac{1}{16\pi} \{ B(s, M_1) \mathcal{F}_{11} \mathcal{G}_{11} + (1 \leftrightarrow 2) \}, \quad (17)$$

where $(1 \leftrightarrow 2)$ indicate the interchange of the indices 1 and 2 and the functions A and B are defined as

$$A(s, M_1, M_2) = \frac{1}{s^2} \int_{-s}^0 dt \frac{(M_1^2 s - 2t(s+t))[t(s+t)\{M_2^2 s - 2t(s+t)\} + M_1^2 \{st(s+t) - M_2^2(s^2 + 2st + 2t^2)\}]}{(t - M_1^2)^2 (t - M_2^2) (M_1^2 + s + t)^2 (M_2^2 + s + t)}, \quad (18)$$

$$B(s, M_i) = \frac{1}{s^2 (s + M_i^2)} \left[s(s + 2M_i^2) + 2M_i^2 (s + M_i^2) \log \frac{M_i^2}{s + M_i^2} \right]. \quad (19)$$

In the limit $s \ll M_1^2, M_2^2$, appropriate for $T_{\text{reh}} \ll M_{1,2}$, we have the simple expressions

$$\sigma_-^s(s) \simeq -\frac{s^2}{64\pi^2} \frac{1}{\Lambda_\varepsilon^6}, \quad \sigma^s(s) \simeq \frac{s}{16\pi} \frac{1}{\Lambda_\sigma^4} \quad (20)$$

for the s -channel case and

$$\sigma_-^t(s) \simeq -\frac{2}{3} \sigma_-^s(s), \quad \sigma^t(s) \simeq \frac{1}{3} \sigma^s(s) \quad (21)$$

for the t channel, where we have introduced the two relevant mass scales $\Lambda_{\varepsilon, \sigma}$:

$$\frac{1}{\Lambda_\varepsilon^6} \equiv \Im[\mathcal{F}_{12} \mathcal{G}_{21}] \left(\frac{\mathcal{F}_{11} + \mathcal{G}_{11}}{M_1^4 M_2^2} - \frac{\mathcal{F}_{22} + \mathcal{G}_{22}}{M_2^4 M_1^2} \right), \quad (22)$$

$$\frac{1}{\Lambda_\sigma^4} \equiv \frac{\mathcal{F}_{11}\mathcal{G}_{11}}{M_1^4} + \frac{\mathcal{F}_{22}\mathcal{G}_{22}}{M_2^4}. \quad (23)$$

Without loss of generality we will choose couplings and masses so that both Λ_ε and Λ_σ are positive. For small couplings, we expect $\Lambda \gtrsim M_i$ and thus generically $T_{\text{reh}} \ll \Lambda_{\sigma,\varepsilon}$ in the limit of interest. Notice that even though one might naively expect $\Lambda_\sigma \ll \Lambda_\varepsilon$, e.g., by considering the hierarchical case $M_1 \ll M_2$ with all couplings of similar order, there are actually enough free parameters here to achieve any desired ratio $\Lambda_\sigma/\Lambda_\varepsilon$ even when perturbative unitarity is taken into account.²

With this, we ultimately find

$$\langle \sigma v \rangle_t \simeq \frac{1}{3} \langle \sigma v \rangle_s \simeq \frac{1}{6} \frac{T^2}{\Lambda_\sigma^4}, \quad (24)$$

$$\varepsilon_t \simeq -2\varepsilon_s \simeq -\frac{12}{\pi} \frac{\Lambda_\sigma^4 T^2}{\Lambda_\varepsilon^6}. \quad (25)$$

The asymmetries decrease with falling temperature, so we can expect the dominant asymmetry generation to occur near the largest temperature, $T \sim T_{\text{reh}}$, corresponding to a UV-freeze-in behavior. Also notice that the asymmetries vanish if only one X_i exists, e.g., via $M_2 \rightarrow \infty$.

With the above proportionalities and $\Sigma_L^{\text{eq}} = 2\Sigma_{e_R}^{\text{eq}} = 2\Sigma_{\nu_R}^{\text{eq}}$ we can simplify the Boltzmann equations to

$$\frac{d\Sigma_{\nu_R}}{dx} = \frac{1}{3\mathcal{H}} \frac{ds}{dx} \langle \sigma v \rangle_t \frac{5}{2} \Sigma_{\nu_R}^{\text{eq}} (\Sigma_{\nu_R} - \Sigma_{\nu_R}^{\text{eq}}), \quad (26)$$

$$\begin{aligned} \frac{d\Delta_{\nu_R}}{dx} = \frac{1}{3\mathcal{H}} \frac{ds}{dx} \langle \sigma v \rangle_t & \left[\frac{5}{2} \Delta_{\nu_R} (\Sigma_{\nu_R} + 3\Sigma_{\nu_R}^{\text{eq}}) \right. \\ & \left. + \frac{1}{4} \varepsilon_t \Sigma_{\nu_R}^{\text{eq}} (\Sigma_{\nu_R} - \Sigma_{\nu_R}^{\text{eq}}) \right]. \end{aligned} \quad (27)$$

We shall assume that the number of relativistic degrees of freedom $g_*(T)$ does not change over the considered range in x which is in particular a good approximation for the Universe before the electroweak phase transition. Accordingly, in the following expressions $g_* = g_*(T_{\text{reh}})$. Equation (26) can then be solved analytically to

$$\Sigma_{\nu_R}(x) = \frac{405\zeta(3)}{4\pi^4 g_*} \left(1 - \exp \left[-\frac{\Gamma}{\mathcal{H}} \frac{x^3 - 1}{x^3} \right] \right), \quad (28)$$

which gives an extremely quickly rising $\Sigma_{\nu_R}(x)$ that then flattens out for $x \gtrsim 2$, see Fig. 2. Here,

²The positive semidefinite nature of \mathcal{F} , \mathcal{G} yields $\Im[\mathcal{F}_{12}\mathcal{G}_{21}] \leq \sqrt{\mathcal{F}_{11}\mathcal{F}_{22}\mathcal{G}_{11}\mathcal{G}_{22}}$. Still this does not restrict $\Lambda_\sigma/\Lambda_\varepsilon$ if one allows for hierarchical entries of \mathcal{F} , \mathcal{G} as well as the masses $M_{1,2}$.

$$\begin{aligned} \frac{\Gamma}{\mathcal{H}} & \equiv 5 \langle \sigma v \rangle_t \frac{\Sigma_{\nu_R}^{\text{eq}}}{6} \frac{1}{\mathcal{H}} \Big|_{T=T_{\text{reh}}}, \\ & \simeq \frac{15\sqrt{5}\zeta(3)}{16\pi^{7/2}\sqrt{g_*}} \frac{M_{\text{Pl}} T_{\text{reh}}^3}{\Lambda_\sigma^4}, \\ & \simeq 0.0044 \left(\frac{106.75}{g_*} \right)^{\frac{1}{2}} \frac{M_{\text{Pl}} T_{\text{reh}}^3}{\Lambda_\sigma^4} \end{aligned} \quad (29)$$

is a measure of interaction strength relative to the Hubble rate $\mathcal{H}(T_{\text{reh}})$. For Eq. (27) we find an excellent approximate solution by assuming a constant $\Sigma_{\nu_R} \simeq \Sigma_{\nu_R}(x \rightarrow \infty)$ on the right-hand side:

$$\begin{aligned} \frac{\Delta_{\nu_R}(x)}{\varepsilon} & \simeq \frac{81\zeta(3)}{8\pi^4 g_*} \frac{\Gamma}{\mathcal{H}} \exp \left[\frac{\Gamma}{\mathcal{H}} \frac{4 - e^{-\frac{\Gamma}{\mathcal{H}}} - x^3}{x^3} \right] \\ & \times \left\{ \frac{E_{-\frac{2}{3}} \left[\frac{\Gamma}{\mathcal{H}} \frac{4 - e^{-\frac{\Gamma}{\mathcal{H}}}}{x^3} \right]}{x^5} - E_{-\frac{2}{3}} \left[\frac{\Gamma}{\mathcal{H}} (4 - e^{-\frac{\Gamma}{\mathcal{H}}}) \right] \right\}, \end{aligned} \quad (30)$$

where $E_n(z) = \int_1^\infty dt t^{-n} e^{-zt}$ is the generalized exponential integral function and we have introduced

$$\varepsilon \equiv \varepsilon_t(T_{\text{reh}}) \simeq -\frac{12}{\pi} \frac{\Lambda_\sigma^4 T_{\text{reh}}^2}{\Lambda_\varepsilon^6} \quad (31)$$

as a convenient measure of CP violation. Similar to Σ_{ν_R} , the generation of Δ_{ν_R} takes place at temperatures close to T_{reh} and quickly approaches a constant value towards larger x .

The numerical solution for the evolution of $|\Delta_{\nu_R}/\varepsilon|$ and Σ_{ν_R} with x is shown in Fig. 2 for three exemplary benchmark points and agrees very well with the analytic approximation above. Note that we employ the approximation of instantaneous reheating, i.e., we assume that all thermal processes relevant for the generation of Σ_{ν_R} and Δ_{ν_R} start at $x = 1$ in a fully thermalized, radiation-dominated Universe with initial conditions $\Sigma_{\nu_R} = \Delta_{\nu_R} = 0$. This assumption is apparently unrealistic but serves as a benchmark scenario to showcase the relevant dynamics. A more realistic reheating phase is expected to introduce $\mathcal{O}(1)$ corrections but does not change the qualitative picture.

Of interest to us are the values of Σ_{ν_R} and $\Delta_{\nu_R}/\varepsilon$ at later times, i.e., at $x \rightarrow \infty$.³ From Eqs. (28) and (30) we find

$$\Sigma_{\nu_R}(\infty) = \Sigma_{\nu_R}^{\text{eq}} (1 - e^{-\Gamma/\mathcal{H}}) \quad (32)$$

with $\Sigma_{\nu_R}^{\text{eq}} = 405\zeta(3)/(4\pi^4 g_*)$ and approximately

$$\frac{\Delta_{\nu_R}(\infty)}{\varepsilon} \simeq \frac{3\Sigma_{\nu_R}^{\text{eq}}}{50} \begin{cases} \frac{\Gamma}{\mathcal{H}}, & \frac{\Gamma}{\mathcal{H}} \ll 1 \\ 2^{-\frac{1}{3}} \frac{5}{24} \Gamma(\frac{5}{3}) (\frac{\Gamma}{\mathcal{H}})^{-\frac{2}{3}} e^{-\frac{\Gamma}{\mathcal{H}}}, & \frac{\Gamma}{\mathcal{H}} \gg 1 \end{cases}. \quad (33)$$

³This is assuming a large separation of T_{reh} and the sphaleron-decoupling temperature $T_{\text{sphaleron}}$, otherwise the relevant quantity is closer to $\Delta_{\nu_R}(T \sim T_{\text{sphaleron}})/\varepsilon$. The asymmetry at that temperature can be much larger but requires a more sophisticated analysis.

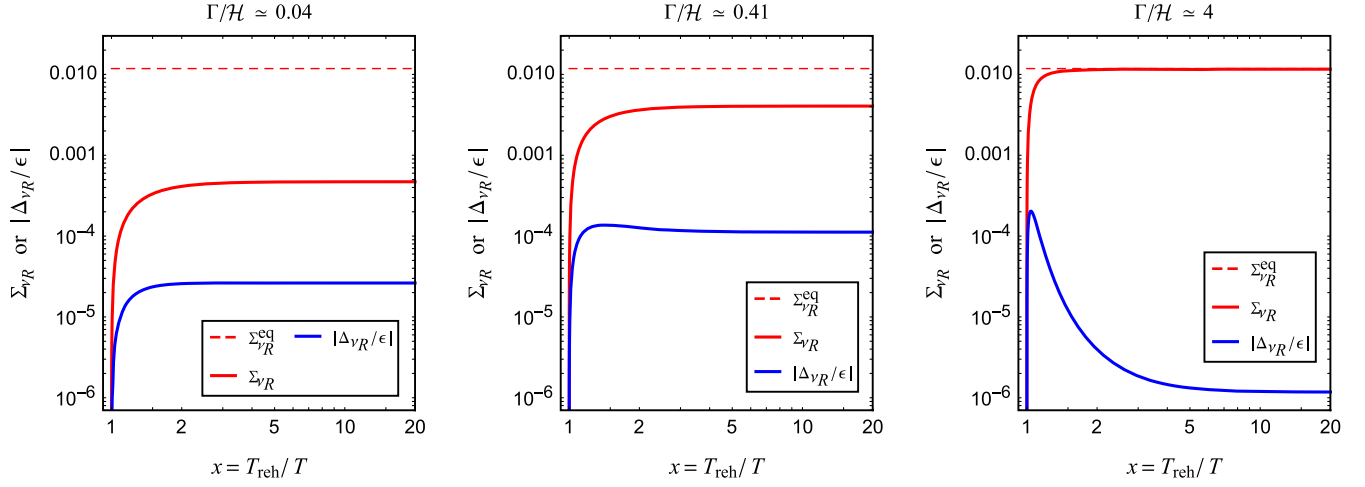


FIG. 2. Evolution of $\Sigma_{\nu_R}(x)$ and $|\Delta_{\nu_R}(x)/\epsilon|$ for three representative parameter points belonging to the freeze-in regime (left panel), maximal $|\Delta_{\nu_R}(\infty)/\epsilon|$ scenario (middle panel) and semithermalized regime (right panel). The dashed red lines show the wouldbe equilibrium distribution of $\Sigma_{\nu_R}(x) = \Sigma_{\nu_R}^{\text{eq}}$, using the high-temperature SM value $g_* = 106.75$.

$\Delta_{\nu_R}(T \sim T_{\text{sphaleron}})/\epsilon$ is directly proportional to the number of effective neutrinos in the early Universe: $\Delta N_{\text{eff}} \simeq 0.14(106.75/g_*)^{4/3} \Sigma_{\nu_R}/\Sigma_{\nu_R}^{\text{eq}}$ (see e.g., Ref. [6]). In Fig. 3, we show ΔN_{eff} as well as the asymmetry $|\Delta_{\nu_R}/\epsilon|$ for large x as a function of Γ/\mathcal{H} . The latter is well approximated by Eq. (33) and takes on a maximal value of $1.1 \times 10^{-4}(106.75/g_*)$ for $\Gamma/\mathcal{H} \simeq 0.41$. This is the sweet spot where many ν_R are produced without thermalizing them. While currently within the experimental limits, CMB-S4 results will be sensitive to ΔN_{eff} down to 0.06 [19,20] and hence probe the region $\Gamma/\mathcal{H} > 0.54$.

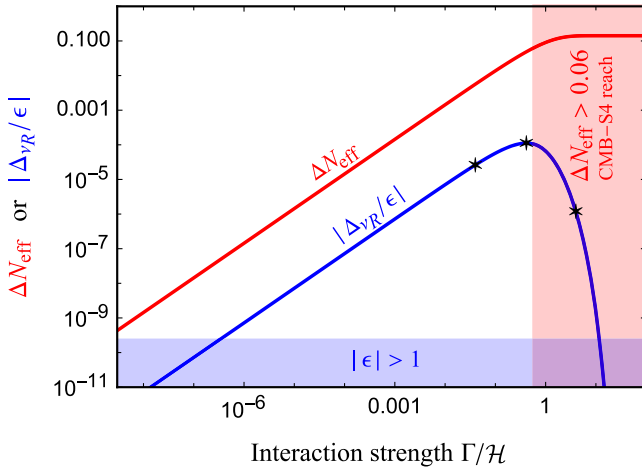


FIG. 3. Numerical solution for $|\Delta_{\nu_R}(\infty)/\epsilon|$ and ΔN_{eff} as a function of Γ/\mathcal{H} in the limit $100 \text{ GeV} \ll T_{\text{reh}} \ll M_1, M_2, \Lambda_\sigma, \Lambda_\epsilon$. The blue shaded region is excluded because it would require an unphysical $|\epsilon| > 1$ to generate the observed baryon asymmetry. The red region gives $\Delta N_{\text{eff}} > 0.06$ and is hence testable at CMB-S4 experiments. The black stars denote the benchmark points shown in Fig. 2.

V. IMPLICATIONS FOR THE BARYON ASYMMETRY

From Eq. (25), we can derive a simple estimate for the baryon asymmetry:

$$|Y_{\Delta B}| \simeq \frac{28}{79} \frac{12}{\pi} \frac{T_{\text{reh}}^2 \Lambda_\sigma^4}{\Lambda_\epsilon^6} \left| \frac{\Delta_{\nu_R}(\infty)}{\epsilon} \right|. \quad (34)$$

We shall focus on the freeze-in regime first, where $\Gamma/\mathcal{H} \ll 1$ and

$$|Y_{\Delta B}| \simeq \frac{0.005}{g_*^{3/2}} \frac{M_{\text{Pl}} T_{\text{reh}}^5}{\Lambda_\epsilon \Lambda_\sigma^5}. \quad (35)$$

Interestingly, the Λ_σ dependence cancels out in $Y_{\Delta B}$ in the freeze-in regime, so Λ_σ controls the interaction rate Γ/\mathcal{H} , while Λ_ϵ controls the asymmetry. We can easily obtain the observed baryon asymmetry with the desired hierarchy $T_{\text{reh}} \ll \Lambda_\epsilon \sim \Lambda_\sigma$,

$$\Lambda_\sigma \simeq \frac{5 \times 10^3 \text{ TeV} [T_{\text{reh}}/\text{TeV}]^{3/4}}{[g_*/106.75]^{1/8} [\Gamma/\mathcal{H}/0.1]^{1/4}}, \quad (36)$$

$$\Lambda_\epsilon \simeq \frac{3 \times 10^3 \text{ TeV} [T_{\text{reh}}/\text{TeV}]^{5/6}}{[g_*/106.75]^{1/4} [Y_{\Delta B}/(9 \times 10^{-11})]^{1/6}}, \quad (37)$$

down to reheating temperatures just above the electroweak phase transition. Since sphalerons decouple below that temperature this is as low as we can go. On the upper end, T_{reh} can be as large as $1.6 \times 10^{18} \text{ GeV}$ ($1.6 \times 10^{12} \text{ GeV}$) before it exceeds $\Lambda_{\sigma,\epsilon}/10$ ($\Lambda_{\sigma,\epsilon}/100$). Notice that we need $\Gamma/\mathcal{H} \gtrsim 4 \times 10^{-7}$ here to keep the $|\epsilon_{s,t}|$ below 1, see Fig. 3.

For $\Gamma/\mathcal{H} > 1$ the asymmetry is exponentially suppressed and we find instead

$$\Lambda_\varepsilon \simeq \frac{2 \times 10^3 \text{ TeV} [T_{\text{reh}}/\text{TeV}]^{5/6} e^{-(\Gamma/\mathcal{H})/6}}{[g_\star/106.75]^{1/4} [Y_{\Delta B}/(9 \times 10^{-11})]^{1/6} (\Gamma/\mathcal{H})^{5/18}}. \quad (38)$$

Here, we need $\Gamma/\mathcal{H} \lesssim 11$ in order to obtain the measured baryon asymmetry with an $|\varepsilon| \leq 1$. Overall, we can explain the baryon asymmetry of our Universe via scattering-induced Dirac leptogenesis for rates $\Gamma/\mathcal{H} \in \{4 \times 10^{-7}, 11\}$; near these end points we require $|\varepsilon| \sim 1$, while in general ε as small as 10^{-6} suffice. Dirac leptogenesis is hence a very efficient mechanism. Our initial assumption $T_{\text{reh}} \ll \Lambda_\sigma, \Lambda_\varepsilon$ is particularly well justified in the case of small reheating temperatures.

Let us briefly mention potential signatures of this model, aside from the Dirac-neutrino nature and potentially enhanced N_{eff} . The above model induces lepton flavor violation, dominantly at one loop in the radiative decay mode $\ell_i \rightarrow \ell_j \gamma$, with branching ratios

$$\text{BR}(\ell_i \rightarrow \ell_j \gamma) = \frac{\alpha_{\text{em}} m_i^5}{144 (16\pi^2)^2 \Gamma_i} \frac{|F_{\alpha i} F_{\alpha j}^*|^2 + |G_{\beta i} G_{\beta j}^*|^2}{4M_X^4}. \quad (39)$$

Here, $\{\alpha, \beta\}$ are summed over the flavor indices $\{e, \mu, \tau\}$. The strongest limits arise in the muon sector, i.e., from $\mu \rightarrow e \gamma$ [21], and reads $|F_{\alpha \mu} F_{\alpha e}^*| < 4 \times 10^{-5} (M_X/100 \text{ GeV})^2$. Assuming no flavor hierarchy in the Yukawa coupling matrices, this limit corresponds to $\Lambda_\sigma > 15 \text{ TeV}$. From Eq. (36) it is clear that Λ_σ will far exceed 15 TeV if we want to explain the observed baryon asymmetry, so we cannot expect any testable lepton flavor violation in this setup.⁴

VI. OTHER MODEL REALIZATIONS

Above we have shown that the simple Dirac-leptogenesis realization of Eq. (1) can give the desired baryon asymmetry even if the mediators X_i are never produced on-shell in the early Universe. This model corresponds to case *a* in Ref. [6] and an analogous discussion can be performed for the other models listed in that reference. Let us briefly discuss one of the models (case *d*), that leads to qualitatively new effects.

Here, the Dirac leptogenesis mediators X are leptiquarks with couplings

$$\mathcal{L} = \bar{d}_R^c F_i d_R X_i + \bar{u}_R^c G_i \nu_R \bar{X}_i + \text{H.c.} \quad (40)$$

This Lagrangian again conserves $B - L$, but violates baryon number. This has two consequences:

- (1) Sphalerons are no longer necessary for the creation of a baryon asymmetry, the scatterings $dd \rightarrow \bar{u}\bar{\nu}_R$ etc. can generate $Y_{\Delta B}$ even for $T_{\text{reh}} < T_{\text{sphaleron}}$, allowing for low-scale baryogenesis.

⁴A possible loophole would be the semithermalized scenario $T_{\text{reh}} \sim T_{\text{sphaleron}}$ mentioned in footnote 3.

- (2) We predict proton decay into ν_R . Assuming there is no flavor hierarchy in the couplings, the rate is approximately determined by Λ_σ :

$$\Gamma(p \rightarrow K^+ \bar{\nu}_R) \simeq \frac{1}{6 \times 10^{33} \text{ yr}} \left(\frac{2 \times 10^{15}}{\Lambda_\sigma/\text{GeV}} \right)^4, \quad (41)$$

so the current limit [22] requires $\Lambda_\sigma > 2 \times 10^{15} \text{ GeV}$. The proton-decay constraint makes it impossible to realize postsphaleron baryogenesis, unlike in the decay scenario of Ref. [6]. Enforcing extreme hierarchies in the leptiquark couplings can suppress proton decay to some degree, e.g., by coupling only to third-generation particles, but it is impossible to evade proton decay entirely [23]. However, in scenarios with a reheating temperature close to its upper limit, leptogenesis works fine potentially with proton-decay signatures around the corner.

Lastly, let us mention that in addition to N_{eff} , lepton flavor violation, and proton decay, other Dirac leptogenesis realizations from Ref. [6] could lead to quark flavor violation while explaining the matter-antimatter asymmetry. Since these depend strongly on the flavor structure of the model these are but qualitative predictions.

VII. CONCLUSION

Dirac leptogenesis exploits the smallness of Dirac-neutrino masses to effectively decouple the right-handed neutrino partners from the SM plasma in the early Universe. With out-of-equilibrium ν_R it is possible to store an asymmetry in this sector that is exactly matched in magnitude by an asymmetry in the SM lepton sector and then converted to a baryon asymmetry by sphalerons. The ν_R asymmetry can be efficiently produced via decays of heavy mediator particles, just like in standard leptogenesis scenarios. In this Letter, we have shown that the non-thermalization of the ν_R is sufficient to satisfy Sakharov's conditions without the need of heavy mediator decays. This makes it possible to obtain the observed baryon asymmetry purely from scatterings without ever producing the mediators. This is relevant for inflationary scenarios with small reheating temperatures compared to the mediator masses. Scattering-induced Dirac leptogenesis makes the same predictions as the decay-induced version: for almost thermalized ν_R we expect an enhanced N_{eff} , potentially in reach of CMB-S4 experiments. Depending on the concrete model, one could also have proton decay, although this can be evaded via hierarchies.

ACKNOWLEDGMENTS

This work was supported in part by the National Science Foundation under Grant No. PHY-2210428. J. Heisig acknowledges support by the Alexander von Humboldt foundation via the Feodor Lynen Research Fellowship for Experienced Researchers and the Feodor Lynen Return Fellowship.

- [1] M. Fukugita and T. Yanagida, Baryogenesis without grand unification, *Phys. Lett. B* **174**, 45 (1986).
- [2] S. Davidson, E. Nardi, and Y. Nir, Leptogenesis, *Phys. Rep.* **466**, 105 (2008).
- [3] V. A. Kuzmin, V. A. Rubakov, and M. E. Shaposhnikov, On the anomalous electroweak baryon number nonconservation in the early universe, *Phys. Lett.* **155B**, 36 (1985).
- [4] A. D. Sakharov, Violation of CP invariance, C asymmetry, and baryon asymmetry of the universe, *Pis'ma Zh. Eksp. Teor. Fiz.* **5**, 32 (1967).
- [5] K. Dick, M. Lindner, M. Ratz, and D. Wright, Leptogenesis with Dirac Neutrinos, *Phys. Rev. Lett.* **84**, 4039 (2000).
- [6] J. Heeck, J. Heisig, and A. Thapa, Testing Dirac leptogenesis with the cosmic microwave background and proton decay, *Phys. Rev. D* **108**, 035014 (2023).
- [7] N. Aghanim *et al.* (Planck Collaboration), Planck 2018 results. VI. Cosmological parameters, *Astron. Astrophys.* **641**, A6 (2020); **652**, C4(E) (2021).
- [8] L. Bento and Z. Berezhiani, Leptogenesis via Collisions: The Lepton Number Leaking to the Hidden Sector, *Phys. Rev. Lett.* **87**, 231304 (2001).
- [9] Y. Cui, L. Randall, and B. Shuve, A WIMPY baryogenesis miracle, *J. High Energy Phys.* **04** (2012) 075.
- [10] K. M. Zurek, Asymmetric dark matter: Theories, signatures, and constraints, *Phys. Rep.* **537**, 91 (2014).
- [11] I. Baldes, N.F. Bell, A.J. Millar, and R.R. Volkas, Asymmetric dark matter and CP violating scatterings in a UV complete model, *J. Cosmol. Astropart. Phys.* **10** (2015) 048.
- [12] A. Ghosh, D. Ghosh, and S. Mukhopadhyay, Cosmology of complex scalar dark matter: Interplay of self-scattering and annihilation, *Phys. Rev. D* **104**, 123543 (2021).
- [13] A. Goudelis, D. Karamitros, P. Papachristou, and V.C. Spanos, Ultraviolet freeze-in baryogenesis, *Phys. Rev. D* **106**, 023515 (2022).
- [14] C.S. Fong, M.C. Gonzalez-Garcia, E. Nardi, and E. Peinado, New ways to TeV scale leptogenesis, *J. High Energy Phys.* **08** (2013) 104.
- [15] D. Aristizabal Sierra, C.S. Fong, E. Nardi, and E. Peinado, Cloistered baryogenesis, *J. Cosmol. Astropart. Phys.* **02** (2014) 013.
- [16] Y. Hamada and K. Kawana, Reheating-era leptogenesis, *Phys. Lett. B* **763**, 388 (2016).
- [17] J.A. Harvey and M.S. Turner, Cosmological baryon and lepton number in the presence of electroweak fermion number violation, *Phys. Rev. D* **42**, 3344 (1990).
- [18] G. Bélanger, F. Boudjema, A. Goudelis, A. Pukhov, and B. Zaldivar, micrOMEGAs5.0: Freeze-in, *Comput. Phys. Commun.* **231**, 173 (2018).
- [19] K. N. Abazajian and J. Heeck, Observing Dirac neutrinos in the cosmic microwave background, *Phys. Rev. D* **100**, 075027 (2019).
- [20] K. Abazajian *et al.*, CMB-S4 science case, reference design, and project plan, [arXiv:1907.04473](https://arxiv.org/abs/1907.04473).
- [21] A. M. Baldini *et al.* (MEG Collaboration), Search for the lepton flavour violating decay $\mu^+ \rightarrow e^+\gamma$ with the full dataset of the MEG experiment, *Eur. Phys. J. C* **76**, 434 (2016).
- [22] K. Abe *et al.* (Super-Kamiokande Collaboration), Search for proton decay via $p \rightarrow \nu K^+$ using 260 kiloton · year data of Super-Kamiokande, *Phys. Rev. D* **90**, 072005 (2014).
- [23] J. Heeck and V. Takhistov, Inclusive nucleon decay searches as a frontier of baryon number violation, *Phys. Rev. D* **101**, 015005 (2020).